JACS
JOURNAL OF THE AMERICAN CHEMICAL SOCIETY
Article
pubs.acs.org/JACS

Precursor Directed Biosynthesis of an Orthogonally Functional Erythromycin Analogue: Selectivity in the Ribosome Macrolide Binding Pocket

Colin J. B. Harvey,[†,∞] Joseph D. Puglisi,[⊥] Vijay S. Pande,[†,∥] David E. Cane,[#] and Chaitan Khosla*[,†,‡,§]

[†]Departments of Chemistry, [‡]Chemical Engineering, [§]Biochemistry, and the [∥]Biophysics Program, Stanford University, Stanford, California 94305, United States

[⊥]Department of Structural Biology, Stanford University School of Medicine, Stanford, California 94035, United States

[#]Department of Chemistry, Brown University, Providence, Rhode Island 02912, United States

Supporting Information

ABSTRACT: The macrolide antibiotic erythromycin A and its semisynthetic analogues have been among the most useful antibacterial agents for the treatment of infectious diseases. Using a recently developed chemical genetic strategy for precursor-directed biosynthesis and colony bioassay of 6-deoxyerythromycin D analogues, we identified a new class of alkynyl- and alkenyl-substituted macrolides with activities comparable to that of the natural product. Further analysis revealed a marked and unexpected dependence of antibiotic activity on the size and degree of unsaturation of the precursor. Based on these leads, we also report the precursor-directed biosynthesis of 15-propargyl erythromycin A, a novel antibiotic that not only is as potent as erythromycin A with respect to its ability to inhibit bacterial growth and cell-free ribosomal protein biosynthesis but also harbors an orthogonal functional group that is capable of facile chemical modification.

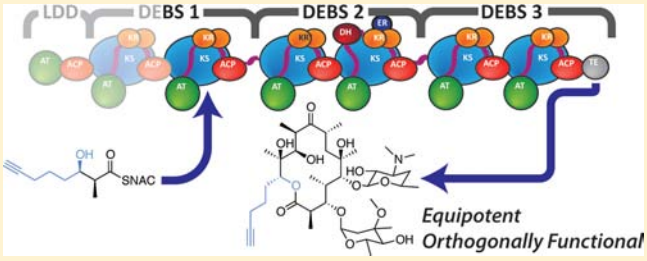

INTRODUCTION

The polyketides are a large class of natural products with clinically important activities ranging from anticancer (doxorubicin) to immunosuppression (FK-506) and, perhaps most prominently, antibacterial. A prototypical polyketide, erythromycin A (**1a**), is produced by the soil bacterium *Saccharopolyspora erythraea* and has been in clinical use as a macrolide antibiotic for more than half a century.[1,2] Its medicinal chemistry has been extensively explored with an eye toward improving its therapeutic potential.[3,4] While these efforts have yielded significant advances, such as the discovery of the second-generation macrolides, clarithromycin and azithromycin, as well as the third-generation ketolide, telithromycin, the intrinsic structural complexity of **1a** has greatly hindered more fundamental variations in the core structure to obtain agents of improved potency and antibacterial spectrum.

Traditionally, alteration of natural product scaffolds has been achieved via semisynthesis or total synthesis. The former approach depends heavily upon modification of the naturally installed functionality. This can be particularly restrictive in the case of **1a**, where regioselectivity is a major challenge. On the other hand, total synthesis of complex natural product analogues is often hampered by practical scalability of a challenging production process. For example, despite extensive efforts by synthetic chemists, there exists to date a single reported total synthesis of **1a**[5−9] and all of the clinically used analogues of the natural product are semisynthetically derived.

Precursor-directed biosynthesis represents a promising alternative to semisynthesis or total synthesis approaches as a means to access analogues of clinically important polyketide natural products.[10,11] This strategy exploits this simplicity of precursors and early intermediates in polyketide biosynthesis by incorporating variants thereof into the corresponding natural product analogue. This approach has been used to synthesize a number of bioactive erythromycin analogues.[12−18]

A major limitation of earlier approaches for polyketide discovery via precursor directed biosynthesis was the scale on which such experiments needed to be conducted. The low conversion efficiency of precursor into product, coupled with challenging fermentation procedures associated with actinomycete bacteria, necessitated the evaluation of alternative synthetic precursors on a relatively large scale in a low-throughput fashion. To circumvent these limitations, we recently engineered an *Escherichia coli* strain that combines the power of precursor directed biosynthesis of erythromycin analogues with the possibilities of a single colony bioassay[19,20] (Figure 1). For example, when a synthetic precursor (**2**) that mimics the natural diketide intermediate in the biosynthesis of 6-deoxyerythronolide B (**3a**, 6-dEB) is fed to a culture of *E. coli*

Received: May 22, 2012
Published: June 28, 2012

   dx.doi.org/10.1021/ja304682q | J. Am. Chem. Soc. 2012, 134, 12259−12265

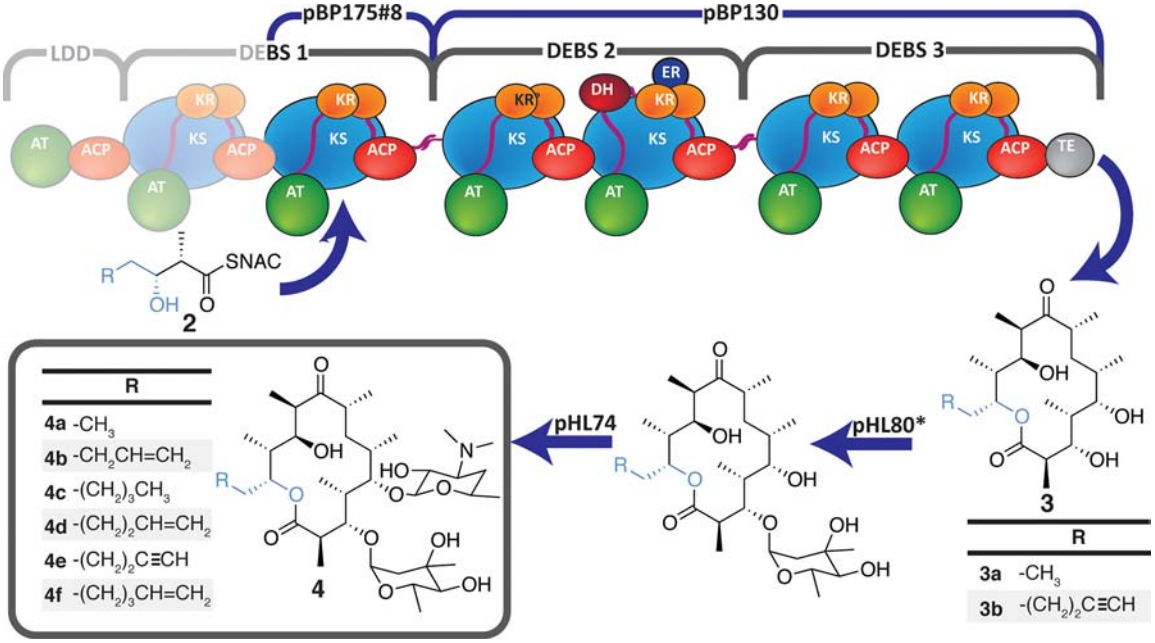

Figure 1. A chemical genetic strategy for rapid discovery of new macrolide antibiotics via precursor directed biosynthesis in *E. coli*. The modular organization of the DEBS assembly line is shown, with each circle representing a distinct active site. The KR domain is shown as a dimer because it consists of an N-terminal structural subdomain and a C-terminal catalytic subdomain. Plasmids pBP175#8 and pBP130 express a truncated derivative of the 6-deoxyerythronolide B synthase (DEBS) lacking the loading didomain and module 1. Plasmids pHL74 and pHL80* express proteins responsible for sugar biosynthesis and glycosyl transfer. Plasmid pBP175#8 also expresses the propionyl-CoA carboxylase genes from *S. coelicolor*. When synthetic diketide **2** is fed to this engineered *E. coli* strain, it is converted into the corresponding 6-deoxyerythromycin D product **4** via the combined action of all of these enzymes.

Table 1. Plasmids and Bacterial Strains Used Throughout This Work

Strain	Description	Plasmid	Gene Products	Strain	Description
Escherichia coli HYL3	A derivative of *E. coli* BAP1 (BL21 Δ*prpRBCD* (*sfp*)) evolved for improved polyketide production.	pBP130	DEBS2-DEBS3	Aglycone biosynthesis	pET21 (carb)
		pBP175#8	PccAB-DEBS Module2	Aglycone biosynthesis	pET28 (kan)
		pHL74	EryCIII-EryCII-TylAI-DesIV-DesI-DesII-DesV-DesVI	TDP-desosamine biosynthesis and transfer	pGZ119 (cm)
		pHL80*	GroES-GroEL-TylCVII-EryBIV-EryBVI-EryBV-TylCIII-EryBII	TDP-mycarose biosynthesis and transfer, Chaperone	pCDF-duet (strep)
Saccharopolyspora erythraea A34	A mutant of *S. erythraea* with a greatly diminished capacity for 6-DEB production	None			
Bacillus subtilis	A representative, macrolide susceptible, gram positive bacterium.	None			

HYL3/pBP130/pBP175#8/pHL74/pHL80* (Table 1), the precursor is converted into the corresponding glycosylated macrolide, 6-deoxyerythromycin D (**4**). The bioactivity of this glycosylated macrolide can be conveniently assayed in a colony assay on a petri dish containing appropriate concentrations of the desired synthetic precursor.

Here, we have used this system to biosynthesize and screen a series of novel erythromycin analogues. Our findings have not only yielded equipotent, orthogonally functionalized analogues of erythromycin A, but also shed light on an unexpected steric relationship in the macrolide binding pocket of the bacterial ribosome.

RESULTS

Precursor Screening. In earlier studies, we described the application of a colony bioassay for the directed evolution of erythromycin biosynthesis in *E. coli*.[19,20] Here, we adapted this assay to evaluate a set of diketide precursors based on the ability of their ultimate biosynthetic product to produce a halo of growth inhibition around single colonies of *E. coli* HYL3/pBP130/pBP175#8/pHL74/pHL80* (Figure 2a,b). As summarized in Table 1, this engineered host-vector system has several features that improve the efficiency of precursor directed biosynthesis. A key advantage of this method for investigating macrolide structure−activity relationships is that it requires only small quantities of a synthetic precursor, thereby enabling analysis of a larger precursor library than possible previously. While this assay is inherently qualitative in nature, owing to its extremely low detection limit it provides a useful tool for the efficient screening and identification of active compounds (Figure 2c).

Several factors were considered when designing the diketides to be screened. Previous work has shown that the stereochemistry of the α-methyl and β-hydroxyl groups, particularly their *syn* orientation, is important for diketide incorporation by module 2.[21] With this in mind, **2b**, the enantiomer of the

dx.doi.org/10.1021/ja304682q | J. Am. Chem. Soc. 2012, 134, 12259−12265

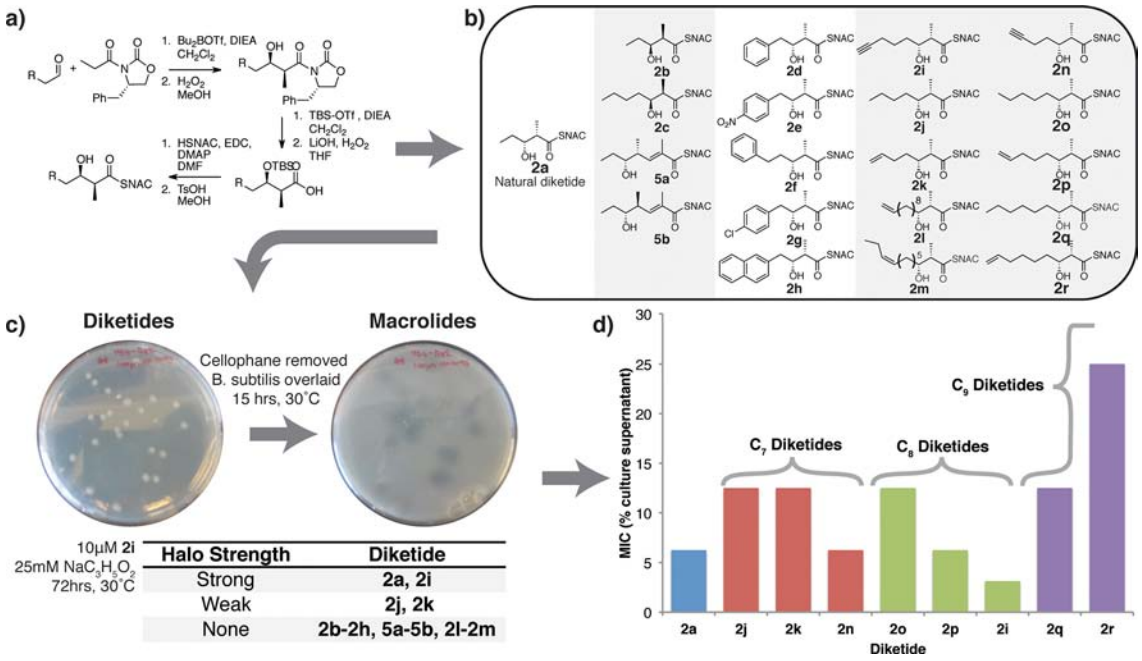

Figure 2. Screening of diketide analogues in a single colony assay. (a) Synthetic route for diketide production (see Supplementary Methods for details). (b) Diketide library. Compounds **2a**−**2m**, **5a**−**b** were used in an initial screen, while compounds **2n**−**2r** were subsequently assayed. None of these diketides themselves had detectable bioactivity. Table S2 illustrates the potential macrolide products of feeding each diketide. (c) Representative petri dish from the initial screening of compound **2i**. Dark halos of growth inhibition can be seen in the *B. subtilis* overlaid lawn, where *E. coli* colonies capable of producing a bioactive compound from the provided precursor had been grown. For the purposes of this work, this was deemed a strong halo. The table summarizes the halo strength from each diketide, classified as a strong, weak, or nonexistent halo. (d) Results from the secondary screen of C_7-, C_8-, and C_9-diketides. The readout of this assay is the minimum amount (% v/v) of a 24-h fermentation culture medium that causes growth inhibition of *B. subtilis*.

natural diketide **2a**, and **2c**, its chain-extended analogue, were the only compounds in which this portion of the precursor was altered. The lack of a growth inhibition halo upon feeding of these latter two diketides is consistent with their expected reduced level of incorporation into the biosynthetic pathway[14] and the fact that the macrolide ring conformation is highly conserved in the crystal structures of most ribosome-bound macrolides.[22,23]

Compounds **5a** and **5b** were also examined, because previous studies showed that these α,β-unsaturated thioesters are processed in unusual ways by DEBS (Scheme S2).[24] Whereas **5a** is recognized as a triketide, presumably due to the *syn*-relationship between the methyl and hydroxyl groups, **5b** is processed as a diketide that is transformed into a 16-membered ring. Perhaps not surprisingly, neither compound gave a detectable halo, presumably because both aglycones are poorly recognized by the necessary glycosyl transferases.

The tolerance of this antibiotic screen for steric bulk was examined by feeding diketides **2d**−**2h**. The benzylated diketide **2d** is known to be transformed by an engineered variant of DEBS into the corresponding erythromycin D analogue, although the bioactivity of this compound is unknown.[13] Therefore, the purpose of feeding **2d**−**2h** was twofold: to test whether or not benzylated **4** was produced at appreciable levels and was sufficiently bioactive to yield a signal, and if so, to determine whether altered electron density (**2e**, **2g**), steric features (**2h**), or flexibility (**2f**) could improve upon this signal. Our data revealed that aromatic functionality at this position of the macrolide is not sufficiently well tolerated to effect detectable growth inhibition (Figure 2c). Of the 14 unnatural diketides tested in this initial screen, only 3 resulted in visible halos: **2i**, **2j**, and **2k**. Of particular interest was the signal produced by **2i**, which was indistinguishable from that produced by **2a**, the natural diketide (Figure 2c). As it is rather unlikely that **2i** would be a better substrate for DEBS KS2 than **2a**, we hypothesized that the corresponding macrolide analogue had bioactivity at least equivalent to that of **4a**. Also notably, both **2j** and **2k**, which were shorter than **2i** by a single methylene and possessed zero or one degree of unsaturation, respectively, produced only weak halos. While these shorter diketides gave diminished signals, **2l** and **2m**, the two initially tested linear precursors longer than **2i**, produced no signal. These results prompted us to examine systematically whether the strong signal seen for **2i** was due to the length and/or the degree of unsaturation of the pendant arm.

A second-generation set of diketides, **2n**−**2r**, were synthesized and screened alongside **2a** as well as **2i**−**2k** in a slightly more sensitive (albeit also qualitative) liquid culture assay (Figure 2d). Two unexpected trends were noted. First, based on the finding that **2n** produced a stronger signal than **2j** or **2k** and **2i** > **2p** > **2o**, the bioactivity resultant from feeding these diketides appeared to be related to their degree of terminal unsaturation. More importantly, the C_8 diketides (**2i**, **2o**, **2p**) gave clearly more active products than either the C_7 or C_9 analogues. We therefore undertook preparative production and isolation of selected macrolide analogues in order to explore their antibacterial properties more rigorously.

Macrolide Analogue Bioactivity. The macrolide 6-deoxyerythromycin D (**4a**) and its analogues (**4b**−**4f**), were isolated from a 5 to 20 L culture of *E. coli* HYL3/pBP130/pBP175#8/pHL74/pHL80*, as described in the Materials and Methods. Their bioactivities were examined against a

dx.doi.org/10.1021/ja304682q | J. Am. Chem. Soc. 2012, 134, 12259−12265

representative Gram-positive bacterium *Bacillus subtilis* (Table 2). These results were, for the most part, consistent with the

Table 2. MIC Values for Selected Macrolide Antibiotics in *B. subtilis* Culture

Compound	MIC in *B. subtilis* culture (nM)
1a	25
1b	25
4a	250
4b	500
4c	500
4d	250
4e	125
4f	2,000
3a	>50,000
3b	>50,000

trend observed in the halo assay. Remarkably, compound **4e** was able to inhibit the growth of *B. subtilis* at a 2-fold lower concentration than the natural product **4a**. Analogue **4d**, where the terminal acetylene was replaced by an olefin, had comparable bioactivity to that of **4a**, whereas the fully saturated analogue **4c** had a 2-fold lower activity. Changing precursor length also had a marked effect on bioactivity, as evidenced by the differences in the antibacterial activities of **4b**, **4d**, and **4f**. Taken together, our findings suggest that substitution at the C-13 position can have an unexpectedly strong influence on macrolide antibiotic activity.

Whereas the identification of an orthogonally functionalized analogue of **4** with improved bioactive properties was encouraging, due to the absence of the 6-OH and 12-OH groups, the macrolides considered to this point were an order of magnitude less active than erythromycin A (**1a** vs **4a** in Table 2). We therefore produced macrolide **1b**, the erythromycin A counterpart of **4e**.

Because there is not yet an efficient *E. coli*-based system capable of direct production of analogues of **1a**, we converted *E. coli* derived 6-dEB (**3a**) and its aglycone analogues into fully decorated macrolide antibiotics using a two-step procedure that has been described previously (Scheme 1).[25]

Scheme 1. Conversion of Diketide 2i into 1b via a two-step procedure

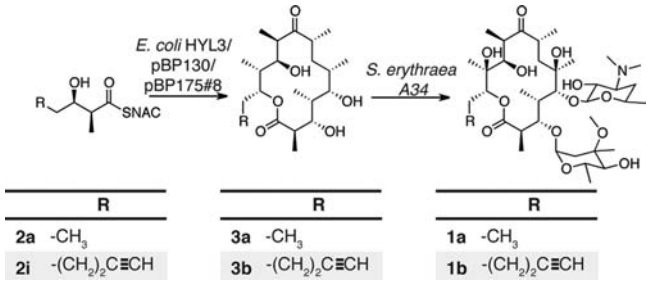

As reported in Table 2, compound **1b** had comparable bioactivity to **1a** with an MIC of 25 nM, a 5-fold improvement on the bioactivity of **4e**. As controls, we confirmed that the aglycones themselves were inactive.

Ribosomal Inhibition. Macrolides act by ribosomal binding and inhibition of protein biosynthesis.[22,26−28] Specifically, **1a** and its semisynthetic analogues bind in the polypeptide exit tunnel of the large ribosomal subunit, thereby occluding passage of the nascent peptide. This causes the translating ribosome to stall and eventually dissociate from the mRNA. We therefore compared the efficacy of **1a** versus **1b** as inhibitors of translation, using a chloramphenicol acetyltransferase cell-free translation system.[29,30] As shown in Figure 3, the inhibitory activities of the two macrolides are equivalent.

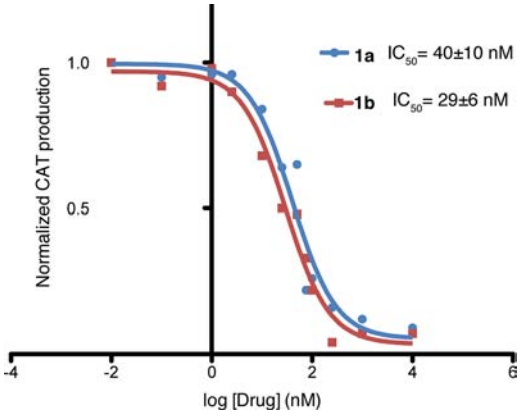

Figure 3. Inhibition of translation by **1a** and **1b** in a cell-free system.

While the macrolide inhibition mechanism described above has been well accepted for some time, the structural details of the macrolide−ribosome interaction have only recently come to light. With the solution of the crystal structures of many prokaryotic ribosomes in the past decade, the ability to probe specific antibiotic interactions through cocrystallization has led to tremendous improvement in the understanding of the mode of action of macrolide antibiotics.[22,23,28,31,32] Using the available crystal structure of **1a** bound to the *E. coli* ribosome[22] we have now developed a structural model to rationalize our structure−activity data by modifying the C-13 substituent of erythromycin A so as to correspond to **1b**. Subsequent minimization of the bound structure using the MMF94 force field resulted in the binding model shown in Figure 4.

Several notable features are apparent from this model. First, despite the complete lack of constraints on the model prior to minimization, very little alteration of the macrocycle conformation is observed (Figure S2). This lack of disruption also extended to the hydrogen bonds formed by the 3″ hydroxyl and tertiary amine of the desosamine moiety, both known to be vital for macrolide function. While all of these key interactions remain intact, the bound structure of **1b** differs from that of **1a** in the orientation of the C-13 substituent. In the case of **1b**, this substituent makes hydrophobic contacts with the wall of the ribosome exit tunnel. In particular, the terminal acetylene is predicted to fit into a groove formed by U746 of the 23S RNA and Lys90 of protein L22. This tight conformational fit might account at least partially for the trend observed in Table 2 since a shorter pendent arm, such as that in **4b**, would not provide such a contact. Conversely, an increase in the length of the substituent such as that in **4f** would likely result in a steric clash with G745.

A comparison of the model for **1b** bound to the ribosome exit tunnel with the crystal structure of telithromycin bound to the same site is shown in Figure 4b. Telithromycin, a recently launched ketolide antibiotic, lacks the cladinose sugar characteristic of all other derivatives of **1**. Its cocrystal structure, in concert with RNA footprinting experiments, has suggested that much of the improved binding affinity could result from the

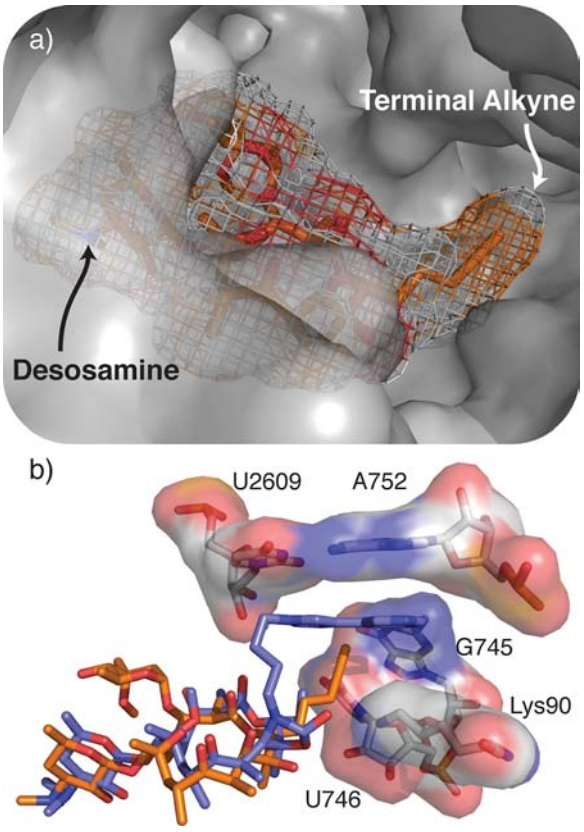

Figure 4. Binding of **1b**. (a) Model of macrolide **1b** docked into the ribosome binding site of **1a**. (b) Modeled structure of **1b** (orange) compared with the experimental crystal structure of telithromycin (blue). The ribosomal residues interacting with the pendant arms are labeled.

strong $\pi-\pi$ stacking interaction between the aryl arm appended to the 11−12 cyclic carbamate and the bridge formed by U2609 and A752. Our model for the ribosomal binding of **1b** suggests that the affinity could be further improved through interaction with the wall of the ribosome exit tunnel. The plethora of facile modifications available via the orthogonally reactive alkyne makes this an attractive and feasible goal.

DISCUSSION

Since the discovery of multimodular polyketide synthases,[33,34] biosynthetic engineers have sought to exploit the assembly line logic of these systems for the production of new and improved antibiotics. Indeed, promising new macrolide antibacterial agents have been prepared through combinations of biosynthetic engineering and medicinal chemical approaches (for example, see Krokidis et al., 2010[35]). Here we have reported the discovery of **1b**, an orthogonally functionalized, equipotent analogue of the widely used macrolide erythromycin A that is directly derived from a fermentation source. In the process, we have uncovered an unexpectedly stringent steric constraint in the portion of the ribosome exit tunnel that accommodates the C-13 ethyl group of **1a.**

The initial motivation for producing bioactive macrolides possessing terminal unsaturation by precursor-directed biosynthesis was the development of a system to facilitate the use of medicinal chemistry for the exploration of the C-13 position. Taken alone, the steric constraint reported here would suggest that **1b** does not fulfill this goal, as any modifications of this position would lead to extension of the pendant arm, a property shown here to diminish bioactivity. Previous reports, however, demonstrate that while the steric constraint reported here holds for linear, unsaturated extensions of the C-13 position, the use of flexible alkyl linkers for appending aromatic heterocycles can lead to greatly improved bioactivity. For example, RNA footprinting studies of one such compound, K-1325 **6** (Figure 5a) bound to the ribosome, have demonstrated that aromatic

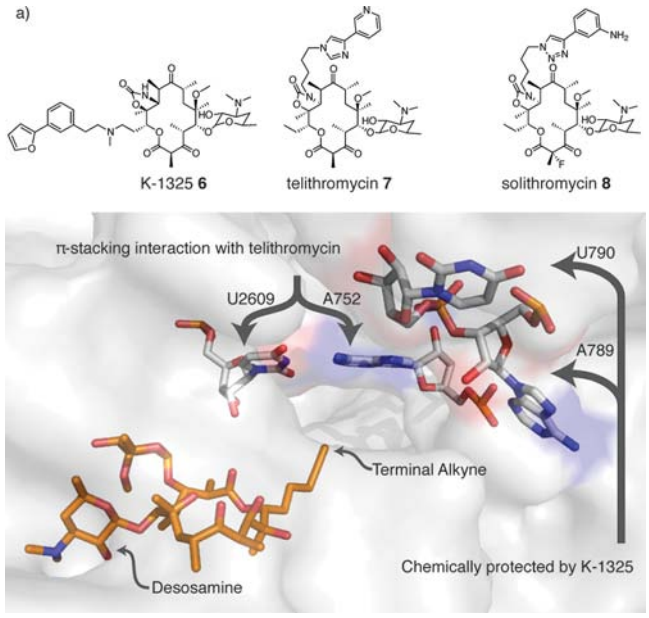

Figure 5. Ketolide binding. (a) Structures of select ketolides. (b) Structure of ribosome bound **1b** compared to residues crystallographically shown to interact with telithromycin and those chemically protected by K-1325.

heterocycles appended by alkyl linkers to the C-13 position of a ketolide led to the strong protection of U790 and A789, two residues within Domain II of the 23S rRNA (Figure 5b).[36] These residues are further down the ribosome exit tunnel, distinct from but proximal to the known interactions of telithromycin **7**, suggesting that modifications to the C-13 position lead to unique constructive interactions as compared to existing macrolides and ketolides. Figure 5b also serves to demonstrate the appreciable volume in the ribosome exit tunnel accessible for further small molecule binding interactions. Taken together, this suggests that while we observe a steric constraint in the series of compounds examined here, this constraint is not absolute and does not obviate the potential of **1b** as a lead for further macrolide development.

Additionally, the installation of triazole-linked aromatic groups is also promising, as this type of functionality on the western portion of the ketolide scaffold is extremely beneficial to bioactivity, as demonstrated by Solithromycin **8** (Figure 5a), a ketolide currently entering phase II clinical development.[37] In the context of these results, **1b** represents a promising lead, which will facilitate future medicinal chemistry efforts by allowing the exploration of a position on the macrolide scaffold that has, to this point, been varied only to a very limited extent.

CONCLUSION

Reported here is the discovery of **1b**, an equipotent and orthogonally functional macrolide antibiotic accessible by

dx.doi.org/10.1021/ja304682q | J. Am. Chem. Soc. 2012, 134, 12259−12265

fermentative means as a promising lead compound for antibiotic development. This discovery serves to reinforce the utility of an engineered *E. coli* based system for rapid and sensitive screening of new macrolide antibiotics, while also demonstrating the power of engineered biosynthesis for the production of new starting materials for anti-infective medicinal chemistry.

MATERIALS AND METHODS

Materials. All solvents used for extraction and purification were ACS grade purchased from Fisher scientific. The synthetic procedures used to prepare diketides **2a**−**2r** have been described previously[12,38] (Figure 2a and Scheme S1). These syntheses were performed using chemicals of the highest available quality from Sigma-Aldrich.

General Methods. All cultures grown in LB broth were supplemented with antibiotics as required at the following concentrations: 100 mg L^{-1} carbenicillin (Teknova, Hollister, CA), 50 mg L^{-1} kanamycin (IBI Scientific, Peosta, IA), 34 mg L^{-1} chloramphenicol (Sigma-Aldrich, St Louis, MO), and 50 mg L^{-1} streptomycin (Santa Cruz Biotechnology, Santa Cruz, CA). Non-standard media used in the growth of *S. erythraea* (V1, F1) are defined in Table S1. Unless otherwise noted, NMR data were collected on a Varian 600 MHz spectrometer (Agilent Technologies, Santa Clara, CA) while HR-MS data were collected using ESI-MS in an Exactive benchtop Orbitrap UPLC-MS (Thermo Scientific, Waltham, MA).

Screening of Diketide Library. Cultures of *E. coli* HYL3/pBP130/pBP175#8/pHL74/pHL80* were grown in LB media overnight to a stationary phase. These cultures were diluted 1000× with LB broth, and 100 μL were plated on cellophane covered LB agar containing 1 mg mL^{-1} sodium propionate and 10−100 μM of the diketide to be tested. These plates were left to incubate at 30 °C for 60 h. The cellophane was then removed, and soft agar containing *B. subtilis* was overlaid. After overnight incubation, the plates were analyzed for halos of growth inhibition where individual colonies of *E. coli* had been located (Figure 2c).

Production of 6-Deoxyerythromycin D Analogues in *E. coli*. Cultures of *E. coli* HYL3/pBP130/pBP175#8/pHL74/pHL80* were grown in LB broth at 37 °C overnight to a stationary phase. These were then used to inoculate larger scale cultures in LB broth (1% v/v), which were grown at 37 °C to OD_{600} = 0.5. The cell pellets were collected by centrifugation (15 min @ 4420*g*) and resuspended at 4 °C in 5% of the original volume of LB media. Cultures were induced by addition of 200 μM β-D-1-thiogalactopyranoside (IPTG) along with the addition of 2.5 g L^{-1} sodium propionate and the desired diketide at 100 μM. This production culture was left to shake at 30 °C for 72 h.

Following this 30 °C incubation, the supernatant was clarified by centrifugation (1 h @ 4420*g*), and 2 M NaOH was added to bring the supernatant pH to 11−12. Extraction with EtOAc (3×), drying over Na_2SO_4, and removal of solvent *in vacuo* resulted in a yellow oil.

Initial purification was performed with acid−base back extraction. The yellow oil was suspended in 10 mL of H_2O, acidified to pH = 2 with 2 M HCl, and extracted with Et_2O (5 × 10 mL). The pH was then adjusted to pH = 12 with 2 M NaOH and extracted with EtOAC (5 × 10 mL). The EtOAc extract was then dried over Na_2SO_4 and the solvent was removed *in vacuo*, yielding a semipure macrolide.

Final purification was performed by HPLC with an RX-C8 column (9.4 mm × 250 mm) from Agilent Technologies (CH_3CN gradient, 0.1% formic acid, 0−25% in 10 min, 25−40% in 80 min, 40−95% in 10 min). The compound identity was verified by NMR (Table S5) and high-resolution mass spectrometry (Table S3).

Production of Analogues of Erythromycin A. These compounds were produced using a two-step procedure (Scheme 1). Cultures of *E. coli* HYL3/pBP130/pBP175#8 were grown in LB media with antibiotics at 37 °C overnight to stationary phase. 1 L cultures in LB media with antibiotics were then inoculated (1% v/v) and left to grow to OD_{600} 0.5 at 37 °C. These cultures were then induced with 200 μM IPTG concomitant with the addition of 200 μM diketide and 2.5 g L^{-1} sodium propionate and left to shake at 18 °C for 72 h. Clarification of the supernatant by centrifugation (1 h at 4420 *g*) was followed by extraction with EtOAc (2 × 1 L per liter culture), drying over Na_2SO_4, and solvent removal *in vacuo*. Partial purification was performed on a silica gel column (10−60% EtOAc in pentane, product $R_f \approx 0.5$ in 50% EtOAc in pentane). This resulted in a semipure yellow oil in which the presence of the 6-dEB analogue was confirmed by NMR.

Conversion of the aglycone into the final antibiotic was performed by microbial transformation in *S. erythraea A34*. All incubations of this strain were performed at 30 °C. Initially, this strain was streaked on a plate of R5 media and left to grow for 72 h. Mycelia were collected and used to inoculate cultures in liquid R5 which were incubated with shaking at for a further 72 h. These cultures were used to inoculate third stage cultures in V2 media (20% v/v), which were left to shake for a further 96 h. V2 cultures were used to inoculate the production culture in an F1 medium (15% v/v). Cultures were incubated for 94 h prior to feeding of the desired 6-dEB analogue (∼25 mg L^{-1} fed as a 50 mg mL^{-1} solution in DMSO). The cultures were monitored daily. When antibiotic production had ceased (5−7 days), the supernatant was clarified by centrifugation (2 h at 4420 *g*), basified to pH 11−12 with 2 M NaOH, and extracted with EtOAc (3 × 500 mL per 500 mL of culture).

Compound purification was performed by HPLC with an RX-C8 column (9.4 mm × 250 mm) from Agilent Technologies (CH_3CN gradient, 0.1% NH_4OH, 5% for 5 min, 5−80% in 150 min, 80−95% in 10 min). The compound identity was verified by NMR (Table S4) and high-resolution mass spectrometry (Table S3)

Measurement of MIC in *B. subtilis* Culture. MIC values were determined through serial dilution in 96-well plates. Compounds are dissolved as 20 μM solutions in DMSO and added to a dilute (0.1% v/v overnight culture) *B. subtilis* culture (1 μM, 5% DMSO v/v). A 2-fold serial dilution down a 96-well plate was performed, and the plate was left to incubate at 30 °C for 20 h. The MIC was defined as the lowest concentration of drug that prevented the OD_{490} of a well from reaching 1.00 (at saturation $OD_{490} \approx 0.2$).

Measurement of Translation Inhibition. The IC_{50} values reported for translation inhibition were measured using a modified version of the PURExpress Δ Ribosome *in vitro* protein synthesis kit (New England BioLabs, Ipswich MA, #E3313). The provided stock ribosomes were diluted to 1 μM with ribosome dilution buffer (RD Buffer: 20 mM HEPES, pH 7.6, 10 mM $Mg(OAc)_2$, 30 mM KCl, 7 mM β-mercaptoethanol). Each reaction was performed on a 10 μL scale with the following components: 3.3 μL of Solution A, 1 μL of factor mix, 0.2 μL of murine RNase inhibitor (NEB #M0314S), 1.5 μL of RD Buffer, 1 μL of ribosome solution (final concentration of 100 nm), 1 μL of nuclease-free water, and 0.5 μL of an antibiotic solution in DMSO (final concentration of 0.1 nM−25 μM). The reactions were initiated by the addition of 80 ng of pUCCAT9L,[39] a plasmid containing the gene for chloramphenicol acetyltransferase (CAT) under the control of a T7 promoter. The reactions were incubated at 37 °C for 2 h, and the production of CAT was assayed spectrophotometrically as follows: 10 μL of reaction mixture were added to 1 mL of assay buffer (100 mM Tris-HCl pH 7.6, 100 μM acetyl CoA, and 0.4 mg mL^{-1} 5,5′-dithiobis(2-nitrobenzoic acid)). The addition of chloramphenicol to a concentration of 100 μM began the reaction, and the change in absorbance at 412 nM was monitored for 5 min.[30,40]

Modeling of Ribosomal Binding. The modeling was based upon the recently solved crystal structure of erythromycin A bound to the ribosome of *E. coli*[22] (PDB ID code 3OFR). The structure of bound **1** was extracted and imported to VIDA (OpenEye scientific software, Santa Fe, NM), where carbon-15 was modified to yield **1b**. This modified structure was then returned to its original biological context, and the modified bound structure was minimized with the MMF94 force field using LigandScout (inte:ligand, Maria Enzersdorf, Austria).

■ ASSOCIATED CONTENT

Supporting Information

Spectroscopic and analytical data, further modeling, and detailed methods. This material is available free of charge via the Internet at http://pubs.acs.org.

■ AUTHOR INFORMATION

Corresponding Author

khosla@stanford.edu

Present Address

[∞]Stanford Genome Technology Center, Department of Biochemistry, Stanford University School of Medicine, Stanford, CA 94305.

Notes

The authors declare no competing financial interest.

■ ACKNOWLEDGMENTS

This research was supported by grants from the National Institutes of Health (GM 087934 to C.K., GM 022172 to D.E.C., GM 51266 to J.D.P., and GM 062868 to V.S.P.). C.J.B.H. is a recipient of a Predoctoral Fellowship from the Center for Molecular Analysis and Design (CMAD) at Stanford University.

■ REFERENCES

(1) *Macrolide Antibiotics: Chemistry, Biology, and Practice*, 2nd ed.; Omura, S., Ed.; Academic Press: Boston, 2002; p 654.

(2) O'Hagan, D. *The Polyketide Metabolites (Ellis Horwood Series in Organic Chemistry)*; Ellis Horwood Ltd.: 1993; p 250.

(3) Ying, L.; Tang, D. *Curr. Top. Med. Chem.* **2010**, *10*, 1441−1469.

(4) Ma, C.; Ma, S. *Mini-Rev. Med. Chem.* **2010**, *10*, 272−286.

(5) Mulzer, J. *Angew. Chem., Int. Ed. Engl.* **1991**, *30*, 1452−1454.

(6) Woodward, R.; Logusch, E.; Nambiar, K.; Sakan, K.; Ward, D.; Au-Yeung, B.; Balaram, P.; Browne, L.; Card, P.; Chen, C; Chenevert, R.; Fliri, A.; Frobel, K.; Gais, H.; Garratt, D.; Hayakawa, K.; Heggie, W.; Hesson, D.; Hoppe, D.; Hoppe, I.; Hyatt, J.; Ikeda, D.; Jacobi, P.; Kim, K.; Kobuke, Y.; Kojima, K.; Krowicki, K.; Lee, V.; Leutert, T.; Malchenko, S.; Martens, J.; Matthews, R.; Ong, B.; Press, J.; Rajan Babu, T.; Rousseau, G.; Sauter, H.; Suzuki, M.; Tatsuta, K.; Tolbert, L.; Truesdale, E.; Uchida, I.; Ueda, Y.; Uyehara, T.; Vasella, A.; Vladuchick, W.; Wade, P.; Williams, R.; Wong, H. *J. Am. Chem. Soc.* **1981**, *103*, 3210−3213.

(7) Woodward, R.; Logusch, E.; Nambiar, K.; Sakan, K.; Ward, D.; Au-Yeung, B.; Balaram, P.; Browne, L.; Card, P.; Chen, C; Chenevert, R.; Fliri, A.; Frobel, K.; Gais, H.; Garratt, D.; Hayakawa, K.; Heggie, W.; Hesson, D.; Hoppe, D.; Hoppe, I.; Hyatt, J.; Ikeda, D.; Jacobi, P.; Kim, K.; Kobuke, Y.; Kojima, K.; Krowicki, K.; Lee, V.; Leutert, T.; Malchenko, S.; Martens, J.; Matthews, R.; Ong, B.; Press, J.; Rajan Babu, T.; Rousseau, G.; Sauter, H.; Suzuki, M.; Tatsuta, K.; Tolbert, L.; Truesdale, E.; Uchida, I.; Ueda, Y.; Uyehara, T.; Vasella, A.; Vladuchick, W.; Wade, P.; Williams, R.; Wong, H. *J. Am. Chem. Soc.* **1981**, *103*, 3213−3215.

(8) Woodward, R.; Logusch, E.; Nambiar, K.; Sakan, K.; Ward, D.; Au-Yeung, B.; Balaram, P.; Browne, L.; Card, P.; Chen, C; Chenevert, R.; Fliri, A.; Frobel, K.; Gais, H.; Garratt, D.; Hayakawa, K.; Heggie, W.; Hesson, D.; Hoppe, D.; Hoppe, I.; Hyatt, J.; Ikeda, D.; Jacobi, P.; Kim, K.; Kobuke, Y.; Kojima, K.; Krowicki, K.; Lee, V.; Leutert, T.; Malchenko, S.; Martens, J.; Matthews, R.; Ong, B.; Press, J.; Rajan Babu, T.; Rousseau, G.; Sauter, H.; Suzuki, M.; Tatsuta, K.; Tolbert, L.; Truesdale, E.; Uchida, I.; Ueda, Y.; Uyehara, T.; Vasella, A.; Vladuchick, W.; Wade, P.; Williams, R.; Wong, H. *J. Am. Chem. Soc.* **1981**, *103*, 3215−3217.

(9) Liu, K.; Kim, H.; Ghosh, P.; Akhmedov, N. G.; Williams, L. J. *J. Am. Chem. Soc.* **2011**, *133*, 14968−14971.

(10) Kennedy, J. *Nat. Prod. Rep.* **2008**, *25*, 25−34.

(11) Kirschning, A.; Taft, F.; Knobloch, T. *Org. Biomol. Chem.* **2007**, *5*, 3245−3259.

(12) Ashley, G. W.; Burlingame, M.; Desai, R.; Fu, H.; Leaf, T.; Licari, P. J.; Tran, C.; Abbanat, D.; Bush, K.; Macielag, M. *J. Antibiot.* **2006**, *59*, 392−401.

(13) Jacobsen, J. R.; Hutchinson, C. R.; Cane, D. E.; Khosla, C. *Science* **1997**, *277*, 367−369.

(14) Jacobsen, J. R.; Keatinge-Clay, A. T.; Cane, D. E.; Khosla, C. *Bioorg. Med. Chem.* **1998**, *6*, 1171−1177.

(15) Goss, R. J. M.; Hong, H. *Chem. Commun. (Camb)* **2005**, 3983−3985.

(16) Desai, R. P.; Rodriguez, E.; Galazzo, J. L.; Licari, P. *Biotechnol. Prog.* **2004**, *20*, 1660−1665.

(17) Frykman, S.; Leaf, T.; Carreras, C.; Licari, P. *Biotechnol. Bioeng.* **2001**, *76*, 303−310.

(18) Shaw, S. J.; Abbanat, D.; Ashley, G. W.; Bush, K.; Foleno, B.; Macielag, M.; Zhang, D.; Myles, D. C. *J. Antibiot.* **2005**, *58*, 167−177.

(19) Lee, H. Y.; Harvey, C. J. B.; Cane, D. E.; Khosla, C. *J. Antibiot.* **2011**, *64*, 59−64.

(20) Lee, H. Y.; Khosla, C. *PLoS Biol.* **2007**, *5*, e45.

(21) Schnarr, N.; Chen, A.; Cane, D.; Khosla, C. *Biochemistry* **2005**, *44*, 11836−11842.

(22) Dunkle, J.; Xiong, L.; Mankin, A.; Cate, J. *Proc. Natl. Acad. Sci. U.S.A.* **2010**, *107*, 17152−17157.

(23) Bulkley, D.; Innis, C. A.; Blaha, G.; Steitz, T. A. *Proc. Natl. Acad. Sci. U.S.A.* **2010**, *107*, 17158−17163.

(24) Kinoshita, K.; Williard, P. G.; Khosla, C.; Cane, D. E. *J. Am. Chem. Soc.* **2001**, *123*, 2495−2502.

(25) Weber, J. M.; Wierman, C. K.; Hutchinson, C. R. *J. Bacteriol.* **1985**, *164*, 425.

(26) Katz, L.; Ashley, G. *Chem. Rev.* **2005**, *105*, 499−527.

(27) Mankin, A. *Mol. Biol.* **2001**, *35*, 509−520.

(28) Tu, D.; Blaha, G.; Moore, P. B.; Steitz, T. A. *Cell* **2005**, *121*, 257−270.

(29) Shimizu, Y.; Inoue, A.; Tomari, Y.; Suzuki, T.; Yokogawa, T.; Nishikawa, K.; Ueda, T. *Nat. Biotechnol.* **2001**, *19*, 751−755.

(30) Shaw, W. V. *Methods Enzymol.* **1975**, *43*, 737−755.

(31) Schlünzen, F.; Harms, J. M.; Franceschi, F.; Hansen, H. A. S.; Bartels, H.; Zarivach, R.; Yonath, A. *Structure* **2003**, *11*, 329−338.

(32) Schlünzen, F.; Zarivach, R.; Harms, J.; Bashan, A.; Tocilj, A.; Albrecht, R.; Yonath, A.; Franceschi, F. *Nature* **2001**, *413*, 814−821.

(33) Cortés, J.; Haydock, S. F.; Roberts, G. A.; Bevitt, D. J.; Leadlay, P. F. *Nature* **1990**, *348*, 176−178.

(34) Caffrey, P.; Bevitt, D. J.; Staunton, J.; Leadlay, P. F. *FEBS Lett.* **1992**, *304*, 225−228.

(35) Krokidis, M. G.; Kostopoulou, O. N.; Kalpaxis, D. L.; Dinos, G. P. *Int. J. Antimicrob. Agents* **2010**, *35*, 235−239.

(36) Kouvela, E. C.; Kalpaxis, D. L.; Wilson, D. N.; Dinos, G. P. *Antimicrob. Agents Chemother.* **2009**, *53*, 1411−1419.

(37) Llano-Sotelo, B.; Dunkle, J.; Klepacki, D.; Zhang, W.; Fernandes, P.; Cate, J. H. D.; Mankin, A. S. *Antimicrob. Agents Chemother.* **2010**, *54*, 4961−4970.

(38) Hartung, I. V.; Rude, M. A.; Schnarr, N. A.; Hunziker, D.; Khosla, C. *J. Am. Chem. Soc.* **2005**, *127*, 11202−11203.

(39) Underwood, K.; Swartz, J.; Puglisi, J. *Biotechnol. Bioeng.* **2005**, *91*, 425−435.

(40) Kim, D. M.; Swartz, J. R. *Biotechnol. Bioeng.* **2001**, *74*, 309−316.